

Spectral study of the Eunomia asteroid family

I. Eunomia [☆]

Andreas Nathues ^{a,*}, Stefano Mottola ^b, Mikko Kaasalainen ^c, Gerhard Neukum ^d

^a Max-Planck-Institut für Sonnensystemforschung, Max-Planck-Straße 2, 37191 Katlenburg-Lindau, Germany

^b DLR, Institute of Space Sensor Technology and Planetary Exploration, Rutherfordstrasse 2, 12489 Berlin, Germany

^c Rolf Nevanlinna Institute, Department of Mathematics and Statistics, P.O. Box 68, 00014 University of Helsinki, Finland

^d Freie Universität Berlin, Institut für Geologie, Geophysik und Geoinformatik, Malteserstraße 74-100, D-12249 Berlin, Germany

Received 11 June 2004; revised 8 December 2004

Available online 19 February 2005

Abstract

We present color ratio curves of the S-Asteroid 15 Eunomia, which have been extracted from high-precision photometric lightcurves obtained in three different VNIR wavelength bands at the Bochum Telescope, La Silla. The measured color ratio curves and near infrared spectra were used to derive a detailed surface composition model whose shape has been computed by V-lightcurve inversions. According to this analysis, the asteroid shows on one hemisphere a higher concentration of pyroxene, which causes an increased 440/700 nm and a reduced 940/700 nm reflectance ratio as well as a pronounced 2- μ m absorption band. The remaining surface shows a higher concentration of olivine, leading to a reduced 440/700 nm and slightly increased 940/700 nm color ratio. In addition, we found that the maximum of the 440/700 nm color ratio curve coincide with the minimum of the 940/700 nm color ratio curve and vice versa. We demonstrate on the basis of USGS laboratory spectra that this anti-cyclical behavior can be explained by choosing Fe-rich olivine and a pyroxene with moderate Fe content as varying mineral phases. Furthermore, our observations confirm that 15 Eunomia is an irregular elongated and at least partially differentiated body. Previous spectral investigations of several smaller fragments of the Eunomia asteroid family revealed that the amount of fragments showing an increased pyroxene content exceeds the amount of pyroxene-poor fragments (Nathues, 2000, DLR Forschungsbericht, ISSN 1434-8454). This finding together with the observation that the major fraction of Eunomia's surface is enriched in olivine let us claim that a large fraction of the original pyroxene-enriched crust layer has been lost due to a major collision that created the Eunomia asteroid family. Significant spectral evidences, consistent with high concentrations of metals have been found neither in the rotational resolved spectra of 15 Eunomia nor in its fragments. This led to the conclusion that either no core consisting mainly of metals exists or that an eventual one has not been unearthed by the impact.

© 2005 Elsevier Inc. All rights reserved.

Keywords: Asteroids; Asteroid composition; Asteroid surfaces; Spectrophotometry; Spectroscopy

1. Introduction

Ground-based astronomical observations use powerful techniques to deliver information on shapes and mineralogical compositions of asteroids. Rotation-induced brightness variations of asteroids are caused by irregular shapes, spectral albedo variations across their surfaces or a combination of both.

The present publication deals with spectro-photometric and spectral observations of Asteroid 15 Eunomia. This study has been conducted in the frame of a doctoral thesis carried out at the DLR, Institute of Space Sensor Technology and Planetary Exploration in Berlin from 1996 to 1999. The primary aim of the project was to ascertain to what extent the largest S-type asteroid of the Solar System, 15 Eunomia, is differentiated in the mineralogical sense. With a diameter of 255 km, Eunomia is also the largest member of the Eunomia asteroid family. Understanding the degree of differentiation of 15 Eunomia is fundamental for constraining existing evolution models of large S-asteroids. Furthermore, the results

[☆] Based on observations carried out at the European Southern Observatory (La Silla, Chile) and Calar Alto Observatory (Spain).

* Corresponding author. Fax: +49-5556-979-139.

E-mail address: nathues@linmpi.mpg.de (A. Nathues).

from this project contribute to the solution of fundamental main-belt evolutionary questions, e.g., the identification of the parent bodies of the ordinary chondrites, the lack of olivine in the asteroid belt and the nature of the M-type asteroids. In order to address these questions both the main body 15 Eunomia and 96 family members were spectrally studied.¹ The fragments in particular permit insights into the internal structure of the parent body.

The Eunomia asteroid family is one of the most numerous known asteroid families in our Solar System (Zappalà et al., 1995). Asteroid families are groups of small bodies whose members exhibit similar “proper elements,” elements, which are corrected for planetary perturbations. Hirayama (1918) (and several subsequent papers) already discovered the most populous and prominent asteroid families, but especially the development of computer power and codes in the last decade led to the identification of more than 20 asteroid families (Williams, 1992; Zappalà et al., 1995). Families identified in this way are called “dynamic” or “nominal” families. Spectral comparisons between individual members suggest that most of them are in fact genetically related, i.e., they are the outcome of catastrophic collisions between minor bodies in the main-belt (e.g., Doressoundiram et al., 1998; Florczak et al., 1998; Lazzaro et al., 1999; Nathues, 2000). The nominal Eunomia family consists of more than 439 asteroids, which show in some cases significant spectral differences among each other (Lazzaro et al., 1999; Nathues, 2000). The majority of these spectral differences are caused by interlopers, i.e., asteroids that are not related to the same parent body, but have by chance similar proper elements.

A complete spectral investigation of an asteroid family includes a detailed spectral examination of its parent body, if it still exists. An appropriate approach is to study the disk integrated spectral behavior of the parent body while it is rotating. Such an investigation enables the detection of compositional variations on a large-area scale across the parent body’s surface, variations, which possibly become also apparent among the individual fragments and hence deliver a more precise picture of the parent body’s nature. For this reason we present results of rotationally resolved color observations and spectra of 15 Eunomia in the following sections.

2. 15 Eunomia

15 Eunomia is the largest S-type asteroid in our Solar System, located in the middle of the asteroid belt (semimajor-axis: 2.644 AU). It has a mean albedo of 0.21 ± 0.03 and its IRAS diameter is 255 ± 15 km (Tedesco et al., 1992). The asteroid shows a retrograde sidereal rotation period of 6.083 hours (Magnusson et al., 1989; Lagerkvist et al., 1989; Kaasalainen et al., 2002a).

Our own precise analysis of several dozens Eunomia lightcurves, obtained over decades by different observers (Lagerkvist et al., 2001), showed that systematic lightcurve features are present. The most prominent features are two different brightness maxima (cp. Fig. 1), which can be explained by an irregular body shape (Gaffey and Ostro, 1987). The difference in the shape of the maxima and other fainter lightcurve residues² could be also the result of spectral albedo variations of the asteroids surface. In the past it was unclear if and to what extent such variations could be present.

Gaffey et al. (1993) classified Eunomia by means of photometric VNIR spectra as S(III)- type. This classification implies a spectrum characterized by signatures of Ca-rich pyroxenes. Olivine and Ni-Fe metal were also identified. This spectral interpretation supports the assumption that Eunomia, or its parent body, were subject of “magmatic” processes. Further mineralogical investigations were carried out by Clark (1995). She derived from her model computations (albedo constrained case) the following surface composition: Olivine (54%), Fe-Ni metal (10%), troilite (19%), and pyroxene (11% Cpx and 5% Opx). We have to bear in mind that this model computation carries a larger uncertainty, since not all features of an S-asteroid spectrum could be modeled correctly. Particular problems occurred in modeling the intense spectral slope between 0.4 and 0.7 μm and the intense change of the spectral slope between 1.5 and 1.6 μm of the S-asteroid spectra with the chosen end-members. Webster and Johnston (1989) examined Eunomia at passive microwaves and concluded the existence of a 1 cm thick surface layer, consisting either of solid porous material with about 10% void space or dust like material. Reed et al. (1997) published rotation-resolved data in thermal and near infrared. Their investigations led to the conclusion that the asteroid body is egg-shaped (with one peaked and one blunt end) and shows a varying surface mineralogy. One part of the surface is dominated by olivine with a higher content of metallic components and less pyroxene (peaked side of the irregular ellipsoid), while the other part of the surface is dominated by iron-rich pyroxenes and a higher general concentration of silicate (blunt end). The authors concluded that 15 Eunomia is the remnant of a stratigraphically structured parent body. Kaasalainen et al. (2002a) recently published a shape model for 15 Eunomia showing a very regular, quasi-ellipsoidal object.

3. Observations

The rotationally resolved relative color photometric observations of 15 Eunomia were carried out in three nights in February 1996 (24th–27th) at the 61 cm Bochum Telescope

¹ The results of the small body spectroscopy will be shown in a further paper.

² Residues: Deviations between the measured lightcurve of an asteroid and the most representative synthetic lightcurve of a rotating triaxial ellipsoid.

(La Silla). The weather conditions were excellent during all nights, often with sub-arcsecond seeing. The telescope was equipped with the DLR MK II camera using a 1024×1024 TK chip and a filter wheel. The color filters b (440 nm),³ w (700 nm), and p (940 nm), all similar to the ECAS survey filters (Tedesco et al., 1982), were used. These filters allow the detection of slope variations of an S-asteroid spectrum between 0.4 and 0.75 μm wavelength and of shape variations of the 1- μm absorption band. The filters were selected sequentially by rotating the filter wheel after each exposure, resulting in three individual color lightcurves per night. The sampling rate was about four minutes for each filter cycle. The chosen exposure times led to signal-to-noise values between 700 and 1100 for 15 Eunomia and always more than 1200 for the reference star, depending on time and used filter.

15 Eunomia was observable for slightly more than 7 h with an airmass value lower than 2, enough to cover continuously more than a full rotation period in each night. Our lightcurve inversions (see section “shape and color computations”) favor the pole solution for the J2000 epoch $\lambda_0 = 2^\circ \pm 5^\circ$, $\beta_0 = -66^\circ \pm 5^\circ$. With this pole position the location of the sub-Earth point on the Eunomia body was calculated to $+8^\circ$ latitude, resulting in an almost complete visibility of the asteroids surface from Earth during our observation campaign.

The star SAO 181024 (spectral type G5, $m_v = 8.7$ mag), located in the same CCD field as Eunomia ($m_v = 10.2$ mag), was used for solar and brightness calibration in the nights 1996 February 24/25 and 1996 February 25/26. In the following night another bright field star ($m_v = 10.44$ mag) had to be used for the brightness calibration. In this case solar spectral calibration has been reached by correcting the color ratio curves by means of the measured color deviations between the field star and SAO 181024. The influence of the spectral differences between SAO 181024 and the Sun are small enough to guarantee appropriate calibration. A comparison with general spectral type investigations by Jaschek and Jaschek (1987) led us conclude that the deviations between SAO 181024 and the solar spectrum are smaller than 2% in b- and w-filter and negligible in p-filter. The photometric reduction of the frames has been performed with AstPhot, a synthetic aperture photometry and astrometry software package developed by SM. Image reduction steps comprised a median bias subtraction, a median skyflat division, and cosmic hit elimination. In order to remove effects induced by the changing airmass from the lightcurves, the previously mentioned calibration stars present in the same CCD field as the asteroid have been used. An aperture of $27''$ diameter was selected to measure the intensity of the asteroid and the star. Differential photometry between asteroid and reference star resulted in lightcurves with an uncertainty be-

tween ± 0.0012 and ± 0.0018 mag, evaluated by considering readout noise, background noise and photon noise. Corrections to the lightcurve data were computed to account for the changing distance between the asteroid and the Sun as well as between the Earth and the asteroid.

The 2.2 m telescope at Calar Alto observatory, equipped with the MAGIC spectrograph, was used in night 30/31 July 1998 to achieve spectra of 15 Eunomia in H- and K-band. The spectrograph uses a 256 by 256 pixel NICMOS detector, which leads to a wavelength resolution of 4 nm pixel^{-1} when using the 1.2 arcsec wide slit. For achieving proper sky removals, the nodding technique according Joyce (1992) has been applied. This technique, in which the object is placed sequentially at certain slit positions, here the A–B–C–A–... nodding sequence along the slit has been used, enables the subtraction of an average sky spectrum, consisting of the $i - 1$ and the $i + 1$ spectral frame, from the individual target spectrum. NIR data reduction steps comprised: (1) subtraction of an averaged sky spectrum from each individual science spectrum, (2) flatfield correction by using a median spectral dome flatfield; such a flatfield was calculated by subtracting a median dark flatfield (lamp OFF) from a median bright flatfield (lamp ON), (3) subtraction of a faint remaining sky background if needed, (4) extraction and alignment of the individual 2-dim target spectra, (5) normalization of each individual target spectrum, (6) calculation of a median over-all target spectrum; this includes cosmic hit and bad pixel filtering, (7) transfer to a 1-dim spectrum, (8) wavelength calibration by using Argon lamp lines and sky lines, (9) calibration for the solar spectrum by using a spectrum of the solar analog star HD 186427 that has been taken at the same airmass as the asteroid. Details of the applied observation techniques and the data reduction processes can be found in Nathues (2000).

4. Lightcurves

The obtained lightcurves of 15 Eunomia are shown in Fig. 1. The zero rotational phase was set to 50137.0 MJD and the duration of a rotation period (1 rp) has been determined to 6.082753 ± 0.000002 h. The lightcurve amplitude between the first maximum (M1) and the second minimum (m2) is larger than between the second maximum (M2) and the first minimum (m1). This amplitude difference was stated to be most probably a result of shape deviations from a triaxial ellipsoidal body (Gaffey and Ostro, 1987). In order to extract precisely the differences between the individual color lightcurves, each has been fitted by a Fourier expansion, also allowing the determination of the lightcurve extrema. A careful comparison between the different color lightcurves shows that the amplitude M1–m2 decreases with increasing wavelength, reaching 0.021 ± 0.002 mag between the filters b and p. In contrast, the amplitude M2–m1 is slightly larger (0.005 ± 0.002 mag) in filter p than in fil-

³ All center wavelengths are a product of the respective filter transmission curve and the CCD sensitivity function. Full width at half maximum of the filter-CCD combinations: b—95 nm, w—100 nm, p—85 nm.

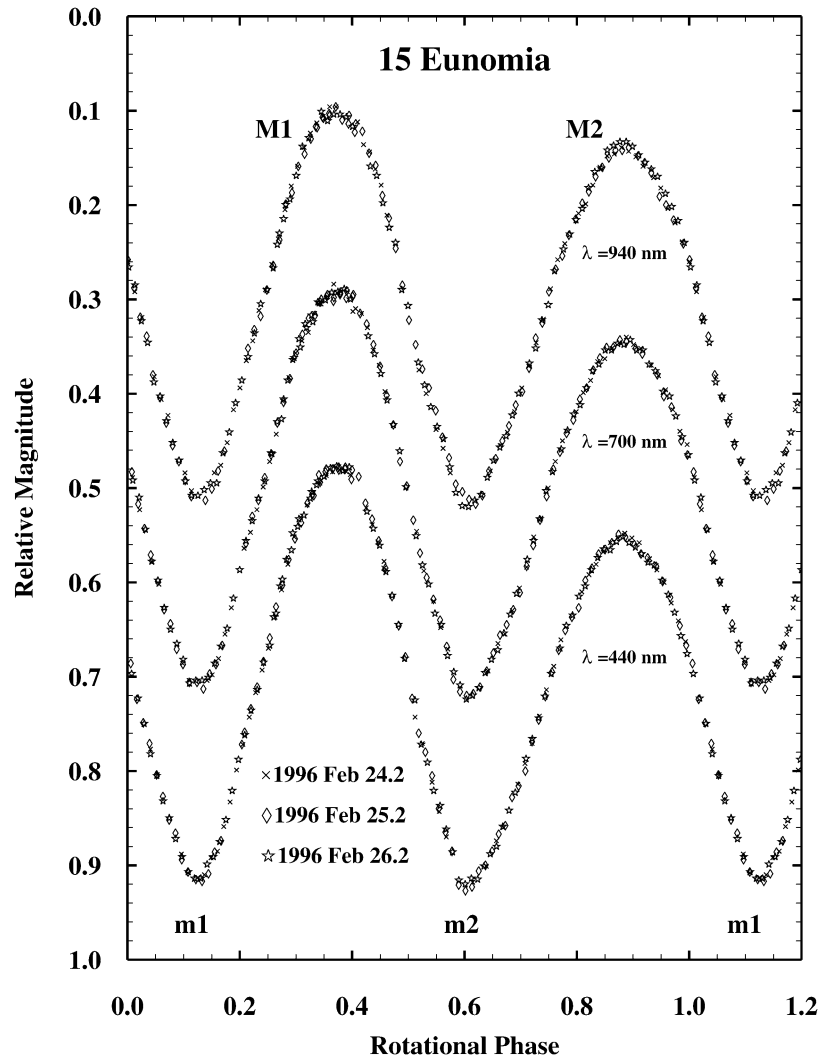


Fig. 1. Nine high precision lightcurves of 15 Eunomia, obtained in three different spectral bands (440, 700, and 940 nm) are shown. The superimposed lightcurves were measured in consecutive nights. Error bars are within the size of the symbols. The w-filter (700 nm) and p-filter (940 nm) measurements are displaced for clarity by -0.2 and -0.4 mag, respectively. The zero rotational phase was set to 50137.0 MJD. Different amplitudes have been identified between the maximum M1 and minimum m2 and the maximum M2 and the minimum m1. Furthermore, the lightcurve amplitude M1–m2 decreases slightly with increasing wavelength (see text for discussion).

ter b. The lightcurves obtained at 700 and 940 nm show a peaked minimum m2 and a rather less peaked minimum m1, showing a difference of 0.007 ± 0.002 mag, when measured from a common reference. The following extrema positions (rp: rotational phase) were determined on the basis of the lightcurve's Fourier expansions:

- 1. Maximum (M1) at 0.376 ± 0.010 rp.
- 1. Minimum (m1) at 0.120 ± 0.010 rp.
- 2. Maximum (M2) at 0.884 ± 0.010 rp.
- 2. Minimum (m2) at 0.610 ± 0.010 rp.

The color ratio curves (Figs. 2 and 3) were extracted in the following way:

Since the measurements in the three filters were not taken simultaneously, we interpolated the w-filter curve by means of a Fourier expansion. This Fourier expansion allowed the

calculation of the w brightness for each instant at which the b- and p-filter points were measured. Then the b and p filter measurement points, scaled in intensities, were divided by the calculated intensities of the reference lightcurve (w-filter). The results, showing the detection of color variations of 15 Eunomia, are displayed in Figs. 2 and 3. The solar calibration of the color ratios was performed on SAO 181024. The color variations between the filters b (440 nm) and w (700 nm), as well as the filters p (940 nm) and w (700 nm) are similar in all three observation nights, indicating real surface color variations and not artifacts introduced by the instrumental or observational technique. The color ratio b/w in Fig. 2 reaches its maximum at 0.358 ± 0.010 rp (ratio: 0.736) and displays a minimum of weaker characteristics between 0.75 and 0.1 rp (ratio: 0.721). The ratio p/w (Fig. 3) achieves its minimum (ratio: 0.978) around 0.321 rp and a weak maximum around 0 rp (ratio: 0.992). A comparison

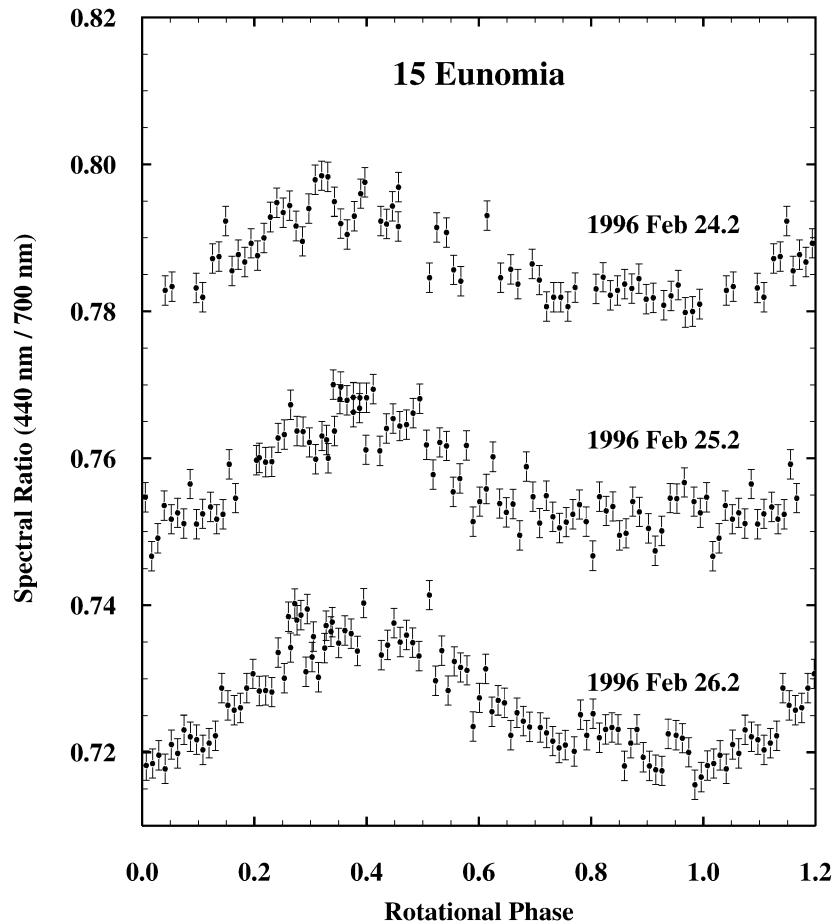


Fig. 2. Displayed is the ratio variation (spectral slope variation shortward of $0.7 \mu\text{m}$) between the lightcurves of the filters b and w in three consecutive nights. The upper ratio curves (1996 February 24 and 1996 February 25) are shifted for clarity by $+0.03$ and $+0.06$, respectively. All nights show the same ratio variation, indicating a real surface color variation. The color ratio maximum at 0.358 ± 0.010 rp is slightly more concise than the minimum between 0.75 and 0.1 rp.

between the color ratio p/w and b/w shows that an anti-phase correlation between both ratios exists. The peak-to-peak amplitude of the ratio b/w is with 0.020 ± 0.002 slightly larger than that of p/w with 0.017 ± 0.004 . Comparisons between the color ratios displayed in Figs. 2 and 3 and spectra of 15 Eunomia from literature (e.g., Lazzaro et al., 1999; Reed et al., 1997) revealed that the color ratio deviations caused by spectral deviations between the respective calibration star and a real solar analog plus the measurement uncertainties amounts to a maximum error of ± 0.02 for the level of the color ratios.

A comparison between the color-ratio curves and the lightcurves shows that the maximum of the ratio curve b/w at 0.358 ± 0.010 rp coincides within its accuracy with the maximum M1 of the rotational light curve (cp. Fig. 1) at 0.376 ± 0.010 rp. The minimum of the color ratio curve p/w at 0.321 ± 0.010 rp is achieved slightly before the lightcurve maximum M1. The M2 is located in the rotational range of the flat minimum of the ratio b/w (0.75 to 0.1 rp) as well as in the beginning of the flat maximum (around 0 rp) of the p/w ratio curve.

The center wavelength positions of the filter—CCD combinations and the shape of the overall Eunomia spectrum between 0.3 and $2.6 \mu\text{m}$ are shown in Fig. 4. The ratio b/w is an indicator for the spectral slope below $0.75 \mu\text{m}$, while the ratio p/w gives an impression about the depth/position of the $1\text{-}\mu\text{m}$ absorption band.

Reed et al. (1997) pointed out that the shape of the 1- and $2\text{-}\mu\text{m}$ absorption band varies with rotation (see Fig. 8). The variations in both absorption bands show according to them a clear correlation. Figure 4 compares one of four similar H- and K-band spectra, which we obtained at nearly identical rotational phases of 15 Eunomia at Calar Alto's 2.2 m telescope, with two photometric spectra of the 52-color survey (Chapman and Gaffey, 1979; McFadden, 1984). The total integration time of the displayed H- and K-band spectrum is 100 s. In Fig. 4 displayed spectra confirm the existence of $2\text{-}\mu\text{m}$ absorption band shape variations.

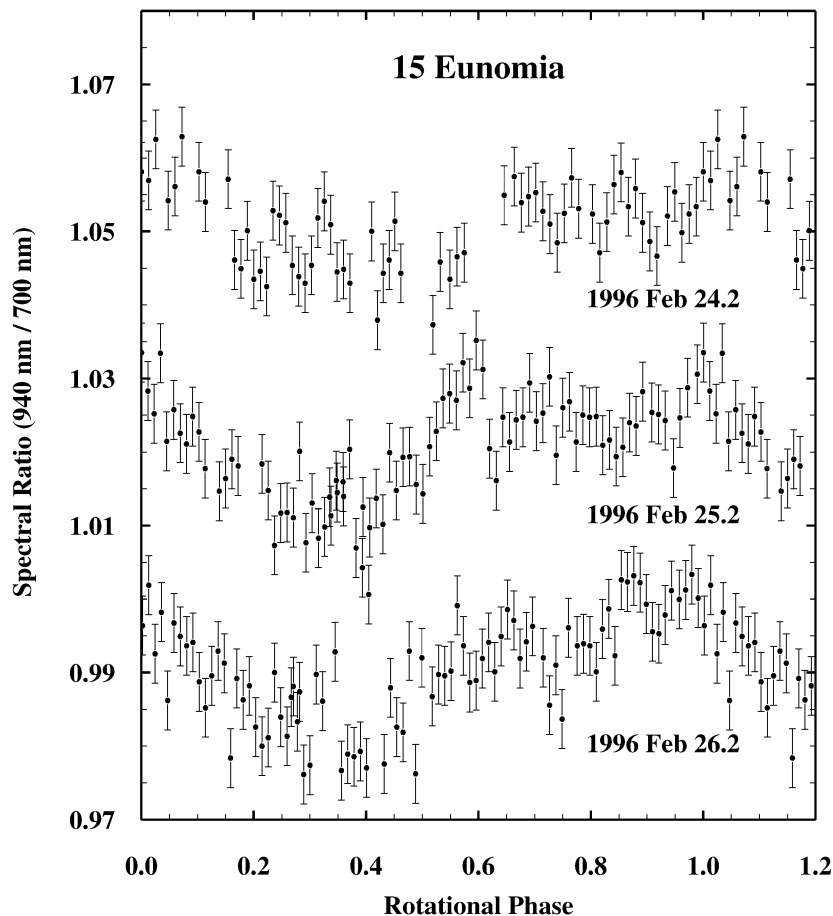


Fig. 3. Displayed is the variation of the color ratio p/w in three consecutive nights. The upper curves (1996 February 24 and 1996 February 25) are shifted for clarity by $+0.03$ and $+0.06$, respectively. Such a variation is the result of changes in the depth and/or changes in the minimum position of the $1\text{-}\mu\text{m}$ absorption band. The weak maximum is reached around 0 rp, while the minimum is being reached at 0.321 ± 0.010 rp.

5. Shape and color computations

By using the color lightcurves reported in this paper, Kaasalainen has refined his previous shape model for 15 Eunomia (Kaasalainen et al., 2002a), which now allows to model the spectral albedo over the surface. The method used for general lightcurve inversion is described in Kaasalainen and Torppa (2001) and Kaasalainen et al. (2001, 2002b). This method makes use of all data points (both relative and calibrated photometry) and finds a physical model with a large number of parameters that accurately reproduces the photometric data down to the noise level. The simultaneously determined parameters describe the sidereal period and the pole direction, the shape, and the light-scattering characteristics of the target. In contrast to the shape model computations in Kaasalainen et al. (2002a) we have used improved input data, since some datasets used in the former paper were unfortunately slightly corrupted due to a minor error in the program that transformed UAPC files (Lagerkvist et al., 2001) into directly usable data format. The error affected the computed observing geometries somewhat sporadically and relatively infrequently. We have found that for

most models the error had a virtually negligible effect, while in a few cases, such as 15 Eunomia, the difference is more visible. The pole solution has changed slightly to ecliptical coordinates $\lambda_0(\text{J2000}) = 2^\circ \pm 5^\circ$, $\beta_0(\text{J2000}) = -66^\circ \pm 5^\circ$ (sidereal period is 6.082753 ± 0.000002 h), and the shape now accurately fits the lightcurves in each detail. The new shape and spin model is also quite similar to the one obtained by combining Hubble Space Telescope's FGS interferometry data with optical lightcurves inversion (Kaasalainen et al., in preparation). The best triaxial ellipsoid approximating the shape solution is 1.6:1.2:1.0. The colored shape model was obtained by first imposing a constant V albedo (as no significant albedo variegation was indicated by the solution mostly based on V -lightcurves), and then allowing the observed b , w and p lightcurves (cp. Fig. 1) to be fitted perfectly using the same shape and pole and changing locally the respective albedoes. With a moderate weight for a regularization function enforcing smoothness of albedo variegation over the surface, this resulted in the model presented in Fig. 5 that explains the observed minor differences in the b , w , and p lightcurves.

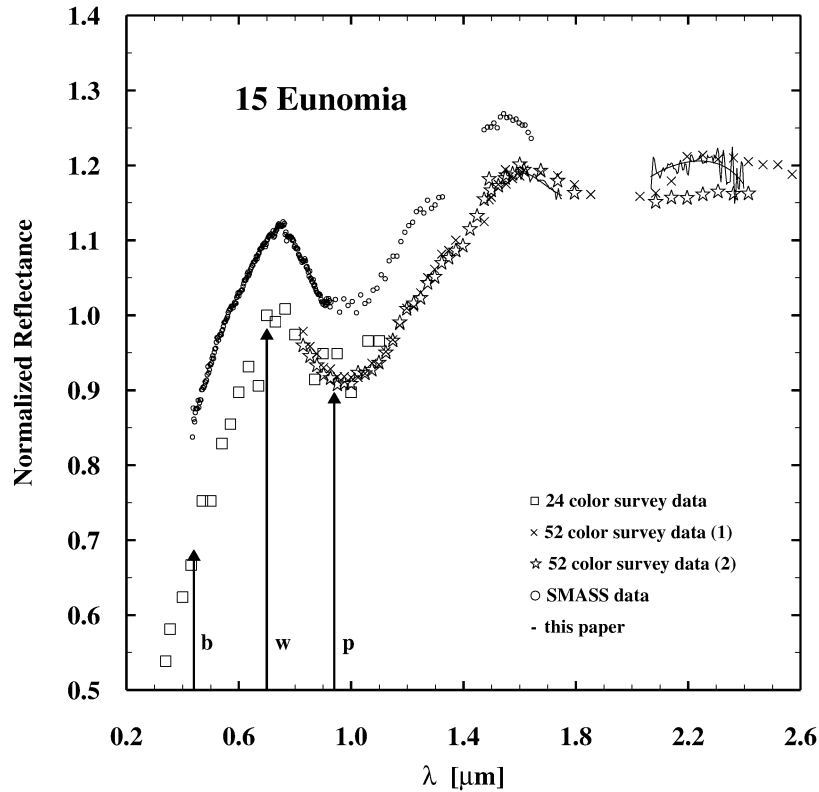


Fig. 4. Reflectance spectra of 15 Eunomia in VNIR wavelengths, normalized at 700 nm. The 24- and 52-color survey data (Chapman and Gaffey, 1979; McFadden, 1984; Bell, 1995) is superimposed by our H- and K-band spectra (a polynomial fit is also shown). The two different 52-color survey spectra are labeled (1) and (2). The VNIR spectrum by Burbine and Binzel (2002), shifted by +0.1 in reflectance for clarity, is also shown for comparison. Number 15 Eunomia is an S-type asteroid with two prominent absorption bands at 1 and 2 μm . The shape of the 2- μm absorption band is different and indicates therefore compositional variations. The center wavelengths of the used filter-CCD combinations (b-, w-, and p-filter) at the Bochum Telescope are marked by arrows.

According to our modeling, the body of 15 Eunomia can be seen as an irregular elongated asteroid showing four sides of different curvature and coloration. The broad side displayed in the upper left picture of Fig. 5 (hereafter referred to as SM1), corresponds to the lightcurve maximum M1 in Fig. 1. This side has a clearly larger curvature radius than the broadside SM2 (third picture from left in the center row). Both ends of the shape model also display different curvatures. The Sm2 side (upper right picture) is slightly more pointed than the Sm1 side (second picture in the last row). In order to display the color ratios, we have chosen a false color representation in which the observed bands are mapped into an RGB space as follows: blue—440 nm, green—700 nm, and red—940 nm. Furthermore, the colors have been raised by a factor 5 to allow a proper visualization. The flatter broadside SM1 is dominated by large bluish areas located at the northern hemisphere, which are responsible for the peak in the color ratio curve b/w in Fig. 2. Some brown tones, indicative of an intensified red fraction, are also present, but are not strong enough to suppress this color ratio peak. In contrast, the broadside SM2 is dominated clearly by brownish facets. These areas are responsible for the weak and flat p/w color ratio plateau in Fig. 3. The short ends Sm1 and Sm2 show on average nearly similar colors, whereby the Sm2 side seems to be a bit more bluish.

6. Discussion

It has been shown in the previous section that although most of the brightness difference between the lightcurve maxima of 15 Eunomia can be explained by the body shape, slight color variations are present on Eunomia's surface.

The color ratio shown in Fig. 2 corresponds to a change of the slope of the Eunomia spectrum in the 0.44 to 0.7 μm wavelength range, while the color ratio shown in Fig. 3 is diagnostic of variations in the 1- μm absorption band. Due to the technique used, however, it is not possible to distinguish whether the observed p/w ratio variation is caused by a shift in the position of the 1- μm absorption band, by a change in its depth or by both.

We should also mention that the color ratios plotted in Figs. 2 and 3 are disk-integrated values, and therefore represent color variations averaged on a hemispheric scale. Therefore the amplitude of the observed variations represents a lower limit for the variations occurring on a local scale. Interestingly enough, the amount of color variation across Eunomia's surface is comprised within the range of color ratios spanned by the nominal S-type members of the Eunomia family (see Fig. 6). This spectral similarity and the subsequent similar mineralogy strengthen the idea that 15

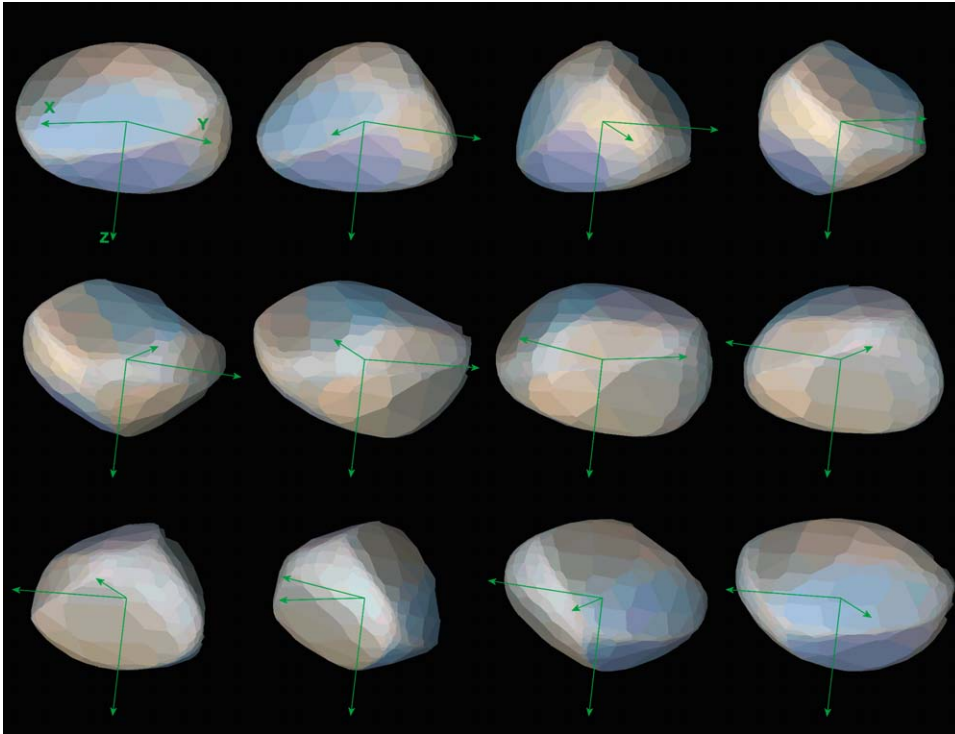


Fig. 5. Color-shape model of 15 Eunomia during one revolution in steps of 30° for 1996 February 24–27. The north pole of the asteroid is down (+Z), while the north pole of the ecliptic is up. False color representation is chosen in which the observed bands are mapped into an RGB space (blue—440 nm, green—700 nm, and red—940 nm). The colors have been raised by a factor of 5. The body shows four different sides: (1) the relatively flat broadside SM1, which is dominated by bluish facets (upper left picture); (2) the “pointed” end sm2, showing several color tones (upper right picture); (3) the more curved broadside SM2 (third picture in center row), which is dominated by brown tones; and (4) the end sm1 which is a bit less bluish and less peaked than sm2 (second picture in the last row). Limb darkening is enabled to reach a better visualization of the shape. The model considers the illumination geometry during the observation campaign (terminator visible at the right borders of the individual pictures).

Eunomia and the smaller S-asteroids of the Eunomia family are genetically related.

Also Reed et al. (1997) have observed hemispheric spectral variation on 15 Eunomia by acquiring NIR spectra at two different rotational phases. In the spectral region where overlap exists, we find a general qualitative agreement between the two data sets, in that both measurements reveal a change in the spectral slope⁴ below $0.75\ \mu\text{m}$ and a variation of the $1\text{-}\mu\text{m}$ absorption band. Furthermore, we confirm spectral differences in the characteristic of the $2\text{-}\mu\text{m}$ absorption, which is diagnostic for the pyroxene content (see Fig. 4).

As mentioned before, the color ratio curves b/w and p/w are in an anti-phase correlation. The presence of a decreasing spectral slope below $0.7\ \mu\text{m}$ and a simultaneous deepening and/or displacement of the $1\text{-}\mu\text{m}$ absorption band exclude two typical explanations for the color ratios we determined:

- (1) Surface albedo variations caused exclusively by grain size variations of the involved phases since this would lead to shallower slopes shortward of $0.7\ \mu\text{m}$ and larger p/w ratios for lower albedo areas (Shkuratov et al., 1999).

- (2) Pure variation in content of a neutral component (e.g., Ni–Fe or iron sulfides) since this would lead to a slope decrease below $0.7\ \mu\text{m}$ and shallower 1- and $2\text{-}\mu\text{m}$ absorption bands (Cloutis et al., 1990). This conclusion, however, does not exclude the presence of a metallic phase. In fact, the characteristics of the absorption bands and the slope of the spectral continuum call for the presence of a metallic phase.

We have calculated the spectral ratios b/w and p/w of each olivine and pyroxene spectrum included in the USGS Digital Spectral Library (Clark et al., 1993) to find a mineralogical explanation for the anti-phase correlation. We searched for pyroxene and olivine spectra showing opposite values for both color ratios and concluded that the anti-phase correlation could be explained by assuming a mixture of these two mineral phases whose relative fraction varies across the asteroid’s surface. Fe-rich olivine (e.g., KI3291, KI3005 or KI3377, Clark et al., 1993), and a pyroxene with moderate Fe content (e.g., Hypersthene PYX02, Clark et al., 1993) would produce the observed spectral variations (cp. Fig. 7), as Fe-rich olivine shows a steeper slope below $0.7\ \mu\text{m}$, while pyroxenes with moderate Fe content show a decreased p/w

⁴ Only partly covered by Reed et al. data.

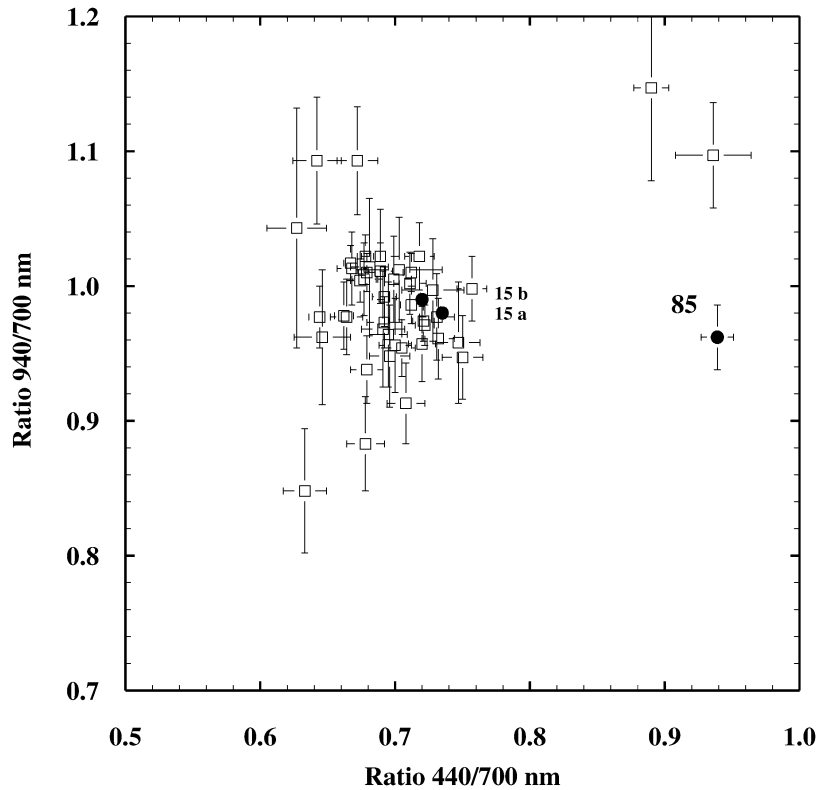


Fig. 6. The spectral color ratios b/w (abscissa) and p/w of several nominal Eunomia family members (Nathues, 2000), are displayed. The color variations detected for 15 Eunomia (filled circles, 15a and 15b represent two spectral extrema) are well within the range of the ratios spread by the small S-type family members. Asteroids that show b/w ratios larger than 0.8 are classified as M- and C-types.

ratio as a result of a 1- μm absorption band minimum, which is shifted to shorter wavelengths.

Beside this compositional influence, the anti-phase correlation could be strengthened by space weathering. Yamada et al. (1999) demonstrated that laser shots on olivine and pyroxene samples led to decreasing b/w ratios and almost constant p/w ratios, whereby olivine samples showed stronger altering than pyroxene samples. Other authors describe a flattening of absorption bands due to space weathering (e.g., Hapke, 2001). Surface areas, which underwent different solar exposure times and/or surface areas of different composition on a hemispherical scale would be needed to explain such a differential spectral darkening. But it is evident that the whole range of the observed spectral variations on 15 Eunomia cannot be explained by differential space weathering alone.

Another explanation could be that the anti-phase correlation is caused by the localized presence of hydrated silicates (having a strong absorption below 0.75 μm and a weak 1- μm absorption) superimposed to a background mainly dominated by anhydrous silicates. However, since it would be surprising to observe native hydrated silicates on an S-type asteroid, this explanation would appear rather unlikely. In this case one would need to invoke an external source for hydrated material as, for example, the result of an impact with a primitive asteroid.

Our conclusion of a varying olivine to pyroxene abundance ratio is also supported by simultaneous changes in the shape of the 1- and 2- μm absorption bands observed by Reed et al. (1997). In addition, Reed et al. presented NIR and thermal lightcurves obtained at 1.6 and 10.2 μm wavelength and concluded, based on slight time shifts between the extrema of the NIR and thermal lightcurves, that surface albedo variations are present on 15 Eunomia. They explained the observed spectral variations by metal and olivine content variations against pyroxene. However, our color measurements confirm olivine but not significant metal variations. Two of the presented spectra in Fig. 4 show a decrease of the reflectance beyond 2.3 μm , which could be an indication for the existence of a Ca-rich clinopyroxene. The spectral variations determined by us are in good agreement with those ones of Reed et al. (1997) and let us conclude that the spectral variations of 15 Eunomia are real and mainly caused by compositional variations across the surface.

Our color ratio plots (Figs. 2 and 3) show the largest color extrema just before reaching the lightcurve maximum M1. This “M1 color deviation” is most likely caused by an enriched pyroxene composition since the b/w color ratio is here maximal while the p/w color ratio is minimal, whereas the other part of the Eunomia body (“background”) is covered by material which shows lower b/w and larger p/w color ratios as a result of an olivine enriched composition. If we compare the rotational phase (rp) in which the

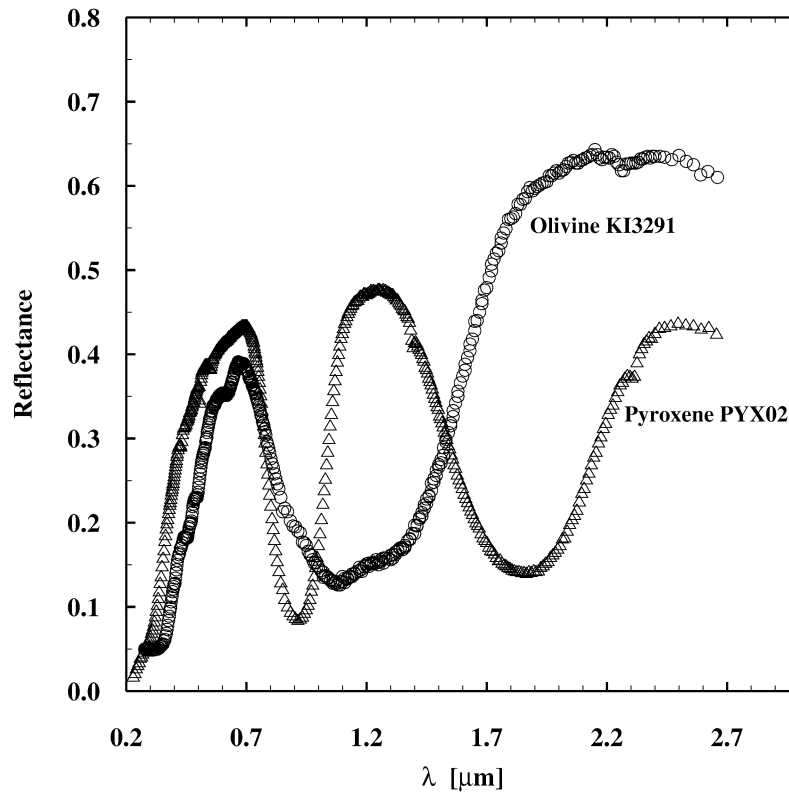


Fig. 7. Spectra of olivine KI3291 and pyroxene PYX02 samples for grain sizes less than $60\ \mu\text{m}$ are shown (Clark et al., 1993). The olivine spectrum displays a steeper slope shortward of $0.7\ \mu\text{m}$ and a $1\text{-}\mu\text{m}$ absorption band minimum that is located at a longer wavelength than those one of the pyroxene spectrum. A mixture of these minerals could explain the anti-phase correlation between the color ratio curves b/w and p/w .

b/w ratio reaches its maximum and p/w reaches its minimum with the rotational phase of the maximum “relative albedo change” found by Reed et al. (1997) then we find a discrepancy of approximately 0.12 rp. The highest relative albedo peak is reached in the Reed et al. data between the minimum $m1$ and maximum $M1$, while our observations show the maximum color difference shortly before reaching the maximum $M1$. Interestingly, the relative albedo starts to rise over the background in the Reed et al. plots just before reaching the lightcurve minimum $m1$, exactly at the same time when our color ratios start to change gradient sign. There is another discrepancy between both observations. Reed et al. assign the maxima of the spectral differences close to the lightcurve minima while our data show the color extrema close to the lightcurve maxima (see Fig. 8). This discrepancy in rotational phase is hardly to explain by phase angle and aspect angle differences between the two sets of observations since these are moderate and very small, respectively. We calculated the maximum difference in aspect to be 0.7° and the phase angle difference to be 8° between our and the Reed et al. observations, using the pole coordinates $\lambda_0 = 2^\circ$, $\beta_0 = -66^\circ$. If the maximum spectral difference is reached between both short ends of the Eunomia body one could argue that the partly different wavelength bands in which the observations were performed are responsible for the observed divergence. This explanation would lead to

the conclusion that 15 Eunomia shows more than four spectrally different regions on hemispherical scale, which seems to be unlikely. Obviously, more VNIR spectra obtained at intermediate rotational phases are necessary to explain this deviation.

When combining our color and shape model (see Fig. 5) with the previous mineralogical allocations we are led to conclude: The Asteroid 15 Eunomia shows an irregular elongated shape and displays slightly different colors across its surface. The varying color is the consequence of a variation of the mineral surface composition. Bluish areas are spectrally characterized by: (1) a larger $440/700\ \text{nm}$ ratio (flatter spectral slope), (2) a lower $940/700\ \text{nm}$ ratio caused by an absorption band minimum, which is shifted to shorter wavelength, and (3) a more pronounced $2\text{-}\mu\text{m}$ absorption band. These spectral characteristics are consistent with a higher pyroxene concentration on the surface. Such a pyroxene enriched composition is mainly found on the broadside SM1 (bluish facets in the upper left picture of Fig. 5). This quasi “pyroxene spot” is surrounded by brownish to pinkish colored facets (increased red fraction), forming a kind of background. The background is spectrally less blue (minor $440/700\ \text{nm}$ ratio), but shows an increased $940/700\ \text{nm}$ ratio due to a $1\text{-}\mu\text{m}$ band minimum, which is shifted to longer wavelength, as well as a less pronounced $2\text{-}\mu\text{m}$ absorption band. These spectral characteristics are indicative for an

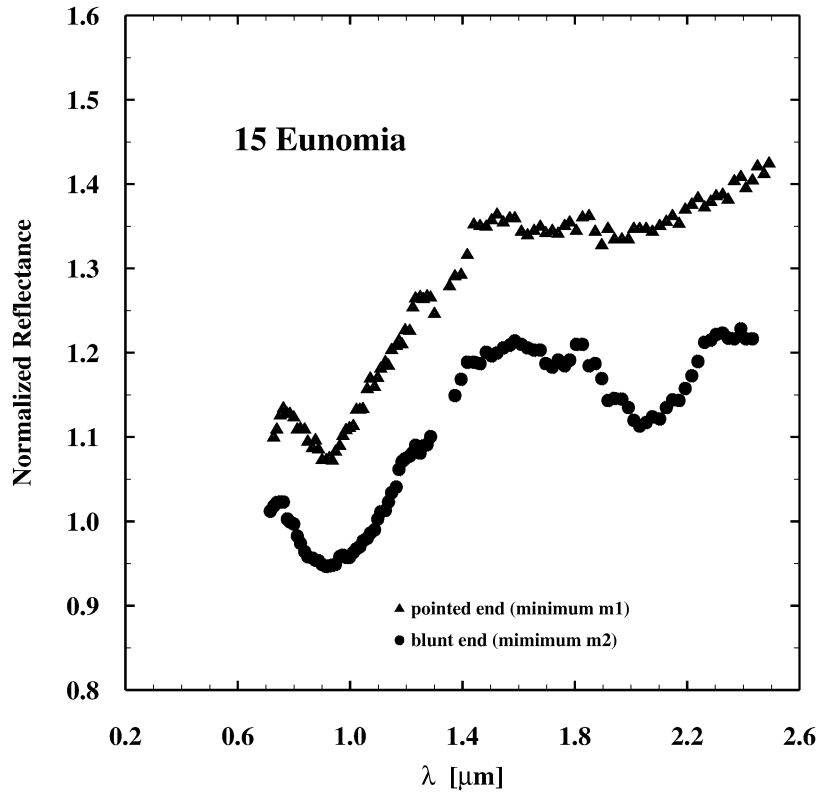


Fig. 8. Spectra of the short ends of Asteroid 15 Eunomia, taken from Reed et al. (1997). The short ends correspond to the lightcurve minima of Fig. 1. The shape of both absorption bands varies.

olivine enriched composition and it seems that the SM2 side (third picture in the center row of Fig. 5) reveals the highest olivine concentration (pinkish and brownish facets), whereas the color distributions of the sides Sm1 and Sm2 are on average similar, possibly with a slightly increased blue fraction on Sm2 (upper right picture of Fig. 5).

The presence of two compositionally different hemispheres confirms that the Asteroid 15 Eunomia is at least partially differentiated. A large fraction of its surface is olivine enriched, while a smaller fraction shows an increased pyroxene content. In addition, observations of almost 100 smaller members of the Eunomia family, believed to represent collisional fragments, display spectral variations in a range that encompasses the spectral variations found across the surface of 15 Eunomia. These spectra show olivine to pyroxene ratio differences among the fragments (Nathues, 2000), and also that the volume of pyroxene enriched material exceeds the volume of pyroxene-poor material. We claim therefore that a large fraction of a former pyroxene-enriched crust layer of 15 Eunomia has been lost due to an impact that generated the Eunomia asteroid family; while exposing at the same time olivine enriched material. The question whether 15 Eunomia has a metalliferous core or not cannot be clarified here. But the discovery of only two possible M-type asteroids among the nominal family members, which have been classified as interlopers (Nathues, 2000), and the fact that the spectra of 15 Eunomia are not dominated by a metallic phase are at

least indications that a core consisting mainly of metals, if such one exist, is unlikely to be exposed.

7. Conclusions

We have investigated the Asteroid 15 Eunomia by means of spectrophotometry and spectroscopy. Rotationally resolved spectrophotometric data were obtained during three nights, each night covering the entire rotation of the body. The derived high precision lightcurves were used to compute a shape and surface composition model of 15 Eunomia. Our main conclusions are:

- (1) We confirm the presence of two compositionally different hemispheres on 15 Eunomia. In the most likely scenario the asteroid shows on one hemisphere a higher concentration of a pyroxene with moderate Fe content, while the remaining surface is dominated by a Fe-rich olivine. Due to this compositional variation, we conclude that 15 Eunomia is at least partially differentiated.
- (2) The asteroid is an irregular elongated body with approximate relative dimensions of 1.6:1.2:1.0. We determined the unambiguous pole solution $\lambda_0 = 2^\circ \pm 5^\circ$, $\beta_0 = -66^\circ \pm 5^\circ$ (J2000) and a sidereal rotation period of 6.082753 ± 0.000002 h.

- (3) Based on the similarities between the color variations across the surface of 15 Eunomia and the color variations among the small members of the Eunomia family, we suggest that a large fraction of the original pyroxene-enriched crust layer of 15 Eunomia has been lost due to a major collision and that a large number of the smaller members are the outcome of this catastrophic event.
- (4) We did not find significant spectral evidences for an eventual existing unearthed metallic core.

Acknowledgments

We thank L. Moroz, A. Erikson, R. Wäsch, U. Mall for fruitful discussions related to this paper.

References

- Bell, J.F., 1995. 52 color asteroid survey, V1.0. <http://pdsbn.astro.umd.edu/sbnhtml/asteroids/spectrophotometry.html>.
- Burbine, T.H., Binzel, R.P., 2002. Small main-belt asteroid spectroscopic survey in the near-infrared. *Icarus* 159, 468–499.
- Chapman, C.R., Gaffey, M.J., 1979. Reflectance spectra for 277 asteroids. In: Gehrels, T. (Ed.), *Asteroids*. Univ. of Arizona Press, Tucson, pp. 655–687.
- Clark, B.E., 1995. Spectral mixing models of S-type asteroids. *J. Geophys. Res.* 100, 14443–14456.
- Clark, R.N., Swayze, G.A., Gallagher, A.J., King, T.V.V., Calvin, W.M., 1993. The U.S. Geological Survey, Digital Spectral Library: Version 1: 0.2 to 3.0 microns. U.S. Geological Survey Open File Report. See also <http://speclab.cr.usgs.gov/spectral.lib04/spectral-lib.desc+plots.html>.
- Cloutis, E.A., Gaffey, M.J., Smith, D.G.W., Lambert, R.St.J., 1990. Metal silicate mixtures: spectral properties and applications to asteroid taxonomy. *J. Geophys. Res.* 95, 8323–8338.
- Doressoundiram, A., Barucci, M.A., Fulchignoni, M., Florczak, M., 1998. Eos family: a spectroscopic study. *Icarus* 131, 15–31.
- Florczak, M., Barucci, M.A., Doressoundiram, A., Lazzaro, D., Angeli, C.A., Dotto, E., 1998. A visible spectroscopic survey of the flora clan. *Icarus* 133, 233–246.
- Gaffey, M.J., Ostro, S.J., 1987. Surface lithologic heterogeneity and body shape for Asteroid (15) Eunomia: evidence from rotational spectral variations and multi-color lightcurve inversions. *Lunar Planet. Sci.* XVIII, 310–311.
- Gaffey, M.J., Bell, J.F., Brown, R.H., Burbine, T.H., Piatek, J.L., Reed, K.L., Chaky, D.L., 1993. Mineralogical variations within the S-type asteroid class. *Icarus* 106, 573–602.
- Hapke, B., 2001. Space weathering from Mercury to the asteroid belt. *J. Geophys. Res.* 106, 10039–10074.
- Hirayama, K., 1918. Groups of asteroids probably of common origin. *Astron. J.* 31, 185–188.
- Jaschek, C., Jaschek, M., 1987. *The Classification of Stars*. Cambridge Univ. Press, Cambridge, ISBN 0521267730.
- Joyce, R.R., 1992. Observing with infrared arrays. In: Howell, S.B. (Ed.), *Astronomical CCD Observing and Reduction Techniques*. ASP Conference Series, vol. 23. Astronomical Society of the Pacific, San Francisco, pp. 258–284.
- Kaasalainen, M., Torppa, J., 2001. Optimization methods for asteroid lightcurve inversion. I. Shape determination. *Icarus* 153, 24–36.
- Kaasalainen, M., Torppa, J., Muinonen, K., 2001. Optimization methods for asteroid lightcurve inversion. II. The complete inverse problem. *Icarus* 153, 37–51.
- Kaasalainen, M., Torppa, J., Piironen, J., 2002a. Models of twenty asteroids from photometric data. *Icarus* 159, 369–395.
- Kaasalainen, M., Mottola, S., Fulchignoni, M., 2002b. Asteroid models from disk-integrated data. In: Bottke, F., Cellino, A., Paolicchi, P., Binzel, R.P. (Eds.), *Asteroids III*. Univ. of Arizona Press, Tucson, pp. 139–150.
- Lagerkvist, C.-I., Harris, A.W., Zappalà, V., 1989. Asteroid lightcurve parameters. In: Binzel, R.P., Gehrels, T., Matthews, M.S. (Eds.), *Asteroids II*. Univ. of Arizona Press, Tucson, pp. 1162–1179.
- Lagerkvist, C.-I., Piironen, J., Erikson, A., 2001. Asteroid Photometric Catalogue, fifth update. Uppsala Univ. Press, Uppsala.
- Lazzaro, D., Mothé-Diniz, T., Carvano, J.M., Angeli, C.A., Betzler, A.S., Florczak, M., Cellino, A., Di Martino, M., Doressoundiram, A., Barucci, M.A., Dotto, E., Bendjoya, P., 1999. The Eunomia family: a visible spectroscopic survey. *Icarus* 142, 445–453.
- Magnusson, P., Barucci, M.A., Drummond, J.D., Lumme, K., Ostro, S.J., Surdje, J., Taylor, R.C., Zappalà, V., 1989. Determination of pole orientations and shapes of asteroids. In: Binzel, R.P., Gehrels, T., Matthews, M.S. (Eds.), *Asteroids II*. Univ. of Arizona Press, Tucson, pp. 66–97.
- McFadden, L.A., 1984. 24-color spectrophotometry. <http://pdsbn.astro.umd.edu/sbnhtml/asteroids/spectrophotometry.html>.
- Nathues, A., 2000. Studie der Eunomia Asteroidenfamilie mittels Spektroskopie (Study of the Eunomia Asteroid family by means of Spectroscopy). DLR Forschungsbericht and Dr. Thesis at Freie Universität Berlin, ISSN 1434-8454.
- Reed, K.L., Gaffey, M.J., Lebofsky, L.A., 1997. Shape and albedo variations of 15 Eunomia. *Icarus* 125, 446–454.
- Shkuratov, Y., Starukhina, L., Hoffmann, H., Arnold, G., 1999. A model of spectral albedo of particulate surfaces: implications for optical properties of the Moon. *Icarus* 137, 235–246.
- Tedesco, E.F., Tholen, D.J., Zellner, B., 1982. The eight-colour asteroid survey: standard stars. *Astron. J.* 87, 1585–1592.
- Tedesco, E.F., Veeder, G.J., Fowler, J.W., Chillemi, J.R., 1992. The IRAS Minor Planet Survey. Philips Lab PL-TR-92-2049, Hanscom Air Force Base, MA.
- Yamada, M., Sasaki, S., Nagahara, H., Fujiwara, A., Hasegawa, S., Yano, H., Hiroi, T., Ohashi, H., Otake, H., 1999. Simulations of space weathering of planet-forming materials: nanosecond pulse laser irradiation and proton implantation on olivine and pyroxene samples. *Earth Planets Space* 51, 1255–1265.
- Webster, W.J., Johnston, K.J., 1989. Passive microwave observations of asteroids. In: Binzel, R.P., Gehrels, T., Matthews, M.S. (Eds.), *Asteroids II*. Univ. of Arizona Press, Tucson, pp. 213–227.
- Williams, J.G., 1992. Asteroid families. An initial search. *Icarus* 96, 251–280.
- Zappalà, V., Bendjoya, P.H., Cellino, A., Farinella, P., Froeschlé, C., 1995. Asteroid families: search of a 12.487-asteroid sample using two different clustering techniques. *Icarus* 116, 291–314.